

Effect of micro-channel geometry on fluid flow and mixing

S. Naher ^a, D. Orpen ^a, D. Brabazon ^a, C.R. Poulsen ^b, M.M. Morshed ^a.

^a Materials Processing Research Centre, Dublin City University, Dublin 9, Ireland

^b Biomedical Diagnostics Institute, Dublin City University, Dublin 9, Ireland

Abstract

Understanding the flow fields at the micro-scale is key to developing methods of successfully mixing fluids for micro-scale applications. This paper investigates flow characteristics and mixing efficiency of three different geometries in micro-channels. The geometries of these channels were rectangular with a dimension of; 300 μm wide, 100 μm deep and 50 mm long. In first channel there was no obstacle and in the second channel there were rectangular blocks of dimension 300 μm long and 150 μm wide are placed in the flow fields with every 300 μm distance attaching along the channel wall. In the third geometry, there were 100 μm wide fins with 150° angle which were placed at a distance of 500 μm apart from each other attached with the wall along the 50 mm channel. Fluent software of Computational Fluid Dynamics (CFD) was used to investigate the flow characteristics within these microfluidic model for three different geometries. A species 2D model was created for three geometries and simulations were run in order to investigate the mixing behaviour of two different fluid with viscosity of water (1 mPa s). Models were only built to investigate the effect of geometry, therefore only one fluid with similar viscosity was used in these models. Velocity vector plots were used in the CFD analysis to visualise the fluid flow path. Mass fractions of fluid were used to analyse the mixing efficiency. Two different colours for water were used to simulate the effect of two different fluids. The results showed that the mixing behaviour strongly depended on the channel geometry when other parameters such as fluid inlet velocity, viscosity and pressure of fluids were kept constant. In two geometries lateral pressure and swirling vortexes were developed which provided better mixing results. Creation of swirling vortexes increased diffusion gradients which enhanced diffusive mixing.

1. Introduction

Microfluidics is the study of fluid flow in geometries with one of the channel dimensions being of the micrometer scale. These geometries are built-up into circuits known as microfluidic chips. This technology has been the cause for much research, as it provides a means for carrying out key chemical assessment processes in the biomedical field [1,2]. This technique has advantages over the standard bench-top method due to the low volume of reagents needed and the higher speed of the analysis [3-5]. Other advantages include the fact that they are readily automated, parallelizable, portable and have relatively low materials cost [6]. This technology has many

application in many different fields including pharmaceuticals, cosmetics, medicine and biotechnology [1,2,6]. Main applications of microfluids at this stage include diagnostics, DNA sequencing, drug delivery, lab-on-a-chip applications, micro-reactors, and fuel cells [1,2,6]. One of the main challenges in microchannel is mixing where more than one fluid come together. It is difficult to get a uniform mixing in microsystem due to the laminar nature of the most micro flow. Various techniques enhance fluid micromixing and their application for biological and chemical processes. One important application of the microfluidic devices is for biological processing where rapid mixing is usually an important step. Besides biological analysis, another application field of the fluid micromixing technology is in microreactor which may bring revolutionary influence on modern chemistry. Roberge and Bieler [7] proposed that 50% of reactions in the fine chemical and pharmaceutical industry could benefit from the continuous process basing on microreactor technology. Micro-reactors will be a good choice for chemists working with very expensive materials or materials only available in small amounts. These will also appeal to users who wish to minimize the risks associated with hazardous materials or reactions by restricting the reactants or products to a minimum. The mixing efficiency of the reactants mainly influences by the reaction time, the yield as well as the quality of the final result. Other parameters in micro-scale flow forces such as tension, interfacial tension and Van der Waal's molecular forces are more apparent than in macro-scale flow [2]. Therefore, it is necessary to research more to understand the fluid flow and appropriate micromixture in microchannel.

The aim of this work is to investigate the behaviour of micromixing in three different geometries of microchannels. The volume fraction of one fluid compare to other fluid were considered to understand the mixing behaviour of two fluids in three different geometries through the channels. Computer simulations were examined by the velocity vectors and flow fields which created by these three geometries within microfluidic systems. The flow patterns have direct effects on resultant mixing pattern and efficiency which were also studied.

2. Model setup

The microchannel structures were created in Gambit which is a pre-processor and an integrated package for CFD analysis. Gambit was used for the discretisation or meshing of the model into finite number of cells. Gambit also used to create geometries meshed and finally exported the mesh files to FLUENT 6.2 for post processing and analysis.

For all microfluidic simulations, the fluid flow is governing by laminar flow patterns due to smaller dimensions. It was chosen for the laminar model in FLUENT solving the species transport equations for the local mass fraction of each species Y_i through the solution of a convection-diffusion equation for the i th species [8]. This conservation equation takes the following general form:

$$\frac{\partial}{\partial t}(\rho Y_i) + \nabla \cdot (\rho \vec{v} Y_i) = -\nabla \cdot \vec{J}_i + R_i + S_i$$

where R_i is the net rate of production of species i by chemical reaction which is ignored in this case. S_i is the rate of creation by addition from the dispersed phase plus any user-defined sources. J_i is the diffusion flux of species i , which arises due to concentration gradients. In this study an equation of this form was solved for two species where v is the total number of fluid phase chemical species present in the system. The flowing assumptions were considered for converging Eq. (1) using the fluent software:

1. The inlet velocity was assumed to be uniform and constant across the inlet cross-section.
2. The system was simplified to contain only the microfluidic channels inlets and outlets.
3. The effects of the fluid solution flowing through the syringe, tubing components and the inlet port of the microfluidic chip were neglected for simplicity of modelling.
4. The exact properties of two fluids were contained in the FLUENT database.
5. Surface roughness of internal walls was considered zero.
6. Gravity was assumed as zero due to the horizontal setup of the microchannels.

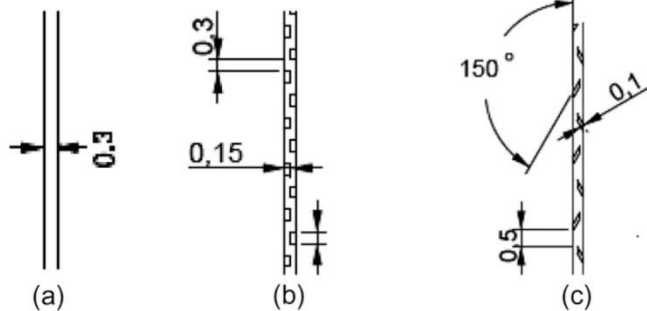
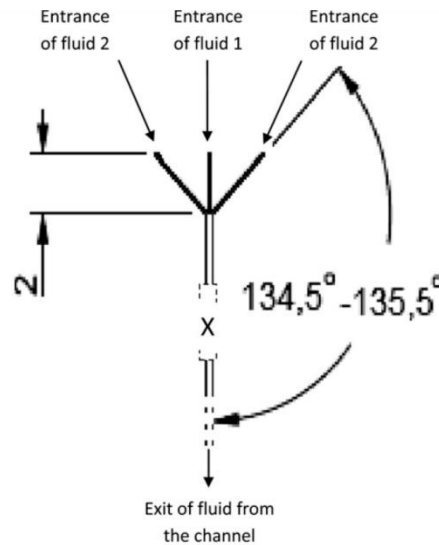


Fig. 1. Top part of this figure represents the common schematic diagram of three different geometries of 50 mm long channel. Figure (a-c) shows detail inside geometry of each channel marked by X on the top sketch. Detail internal configuration of Geometry 1 is in (a), Geometry 2 is in (b) and Geometry 3 is in (c); all dimensions are in mm.

Fig. 1 shows the schematic diagram of three different geometries which were considered for this simulation. All three channels are 50 mm long and 0.3 mm diameter with three inlets of each 0.1 mm diameter. Geometry 1 has a simple straight channel (Fig. 1 a). Geometry 2 has uniform blocks throughout the channel (Fig. 1 b) and Geometry 3 has upward fins along the channel (Fig. 1c).

The model geometries were meshed using GAMBIT 2.4.6. Face meshing was used to get a range of element/scheme type combinations of quadrilateral and triangle [9]. Meshes with 200,000-20,00,000 nodes are commonly used in these geometries. The boundary conditions such as velocity in and pressure outlet, channel walls were assigned to the appropriate boundary zones. On the inlet boundary, the condition of "mass flow inlet" was used. The inlet was defined as a mass flow inlet. This was done so that a uniform mass flow could be assigned across the whole of the inlet boundary similar to how an actual microchannel inlet would behave experimentally. This was done by neglecting the walls which were setup to include a no-slip condition. The outlet was defined as a pressure outlet, this meant that the pressure at the outlet could be computed relative to the set conditions and the amount of opposition to the direction of flow the system presented could be easily observed. A "pressure outlet" was defined at the outlet so that a target outflow could be set so that solutions would converge more accurately and quicker. All other lines are set by Gambit to the default of wall. The operating pressure was kept to the default of atmospheric pressure.

Two different colour of water was chosen to identify the mixing behaviour in the channels. Setting of the under relaxation forces were moved from the default 1 to 0.95 to makes it easier for the solution to converge. Here fluid 1 designated as yellow whereas fluid 2 was designated as sky blue colour. Table 1 shows the water properties which was used for running the simulation through the channels. The two outer inlets are supplying fluid 2 to the system and the central inlet is supplying fluid 1 (Fig. 2). All three inlets have the same flow rate of 100 ml/min. This means that once the system is fully mixed, it will have 0.3333 mass fraction of fluid 1 and 0.666 mass fraction of fluid 2.

Property	Value
Density (kg/m)	989.2
Cp (J/kg k)	4182
Thermal conductivity (W/m k)	0.6
Viscosity (kg/m s)	0.001
Molecular weight (kg/kg mol)	18.0512
Standard state entropy (J/kg mol)	69902.2
Reference temperature (K)	298
Vaporising temperature (K)	284
Boiling point (K)	373
Saturation vapour pressure (Pa)	2658
Droplet surface tension (n/m)	0.07194

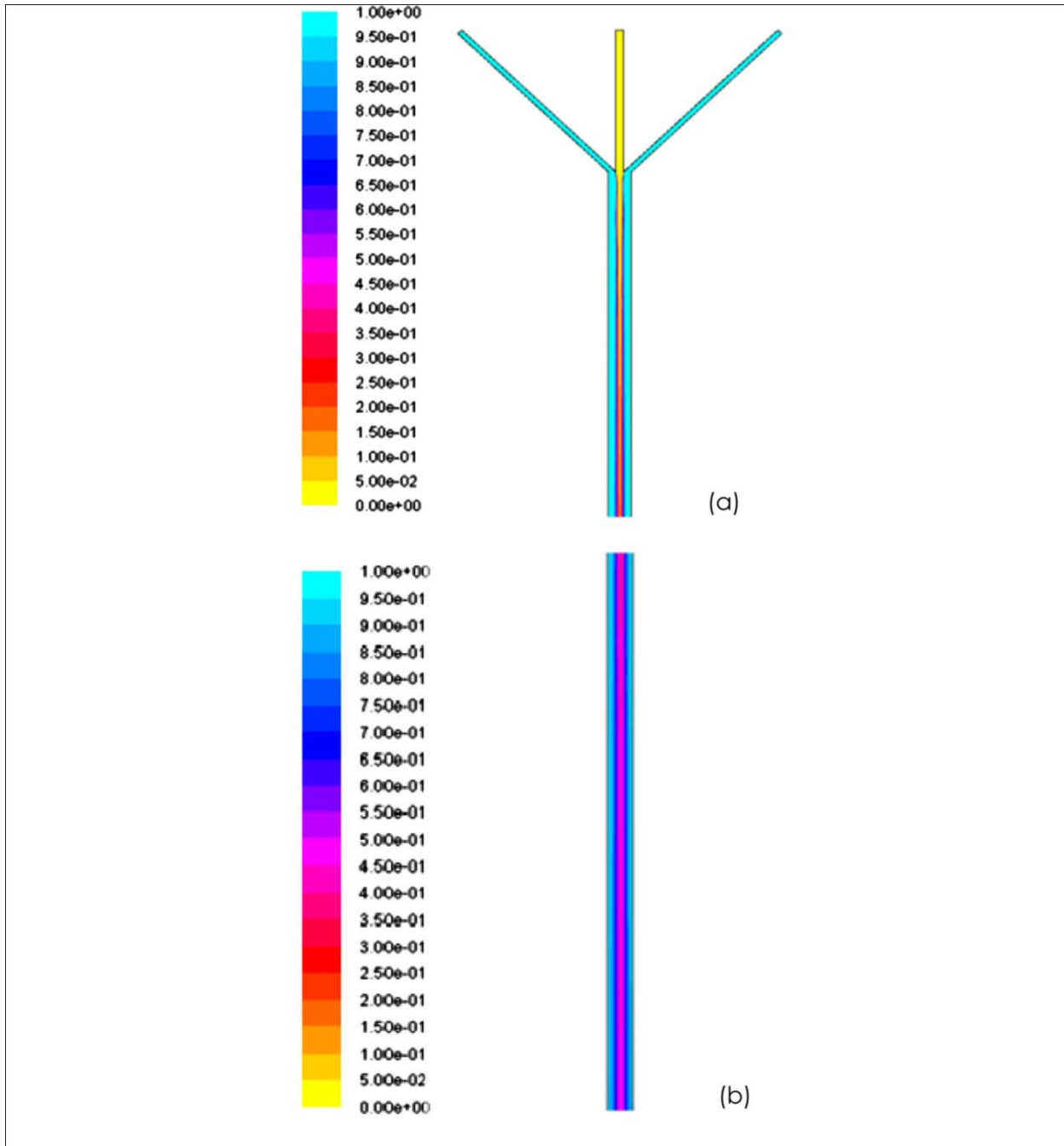


Fig. 2. Fluent results along the channel for Geometry 1, (a) in the entrance of the channel and (b) at the exit of the channel. Scale bar for mass fraction fluid 1 and fluid 2 are shown in the left.

3. Results and discussion

The simulation results presented with mass fraction of fluids 1 and 2 in the inlet and the outlet sections of mixing channel for three geometries are shown in Figs. 2-4. The amount of one fluid compared to other fluid throughout the model provided a general picture of the mixing taking place. Fig. 2a and b shows that there is no mixing achieved through the channel. This is because

of typical laminar flow in the channel and no swirling or vortex formation during the fluid flow. Fig. 3a and b has block effect inside the channel. Blocks are one of the most frequently used geometries in microfluidic for creating vortex [10]. In Geometry 2, the mixing starts at a distance at around 45 mm of the channel length from the inlet.

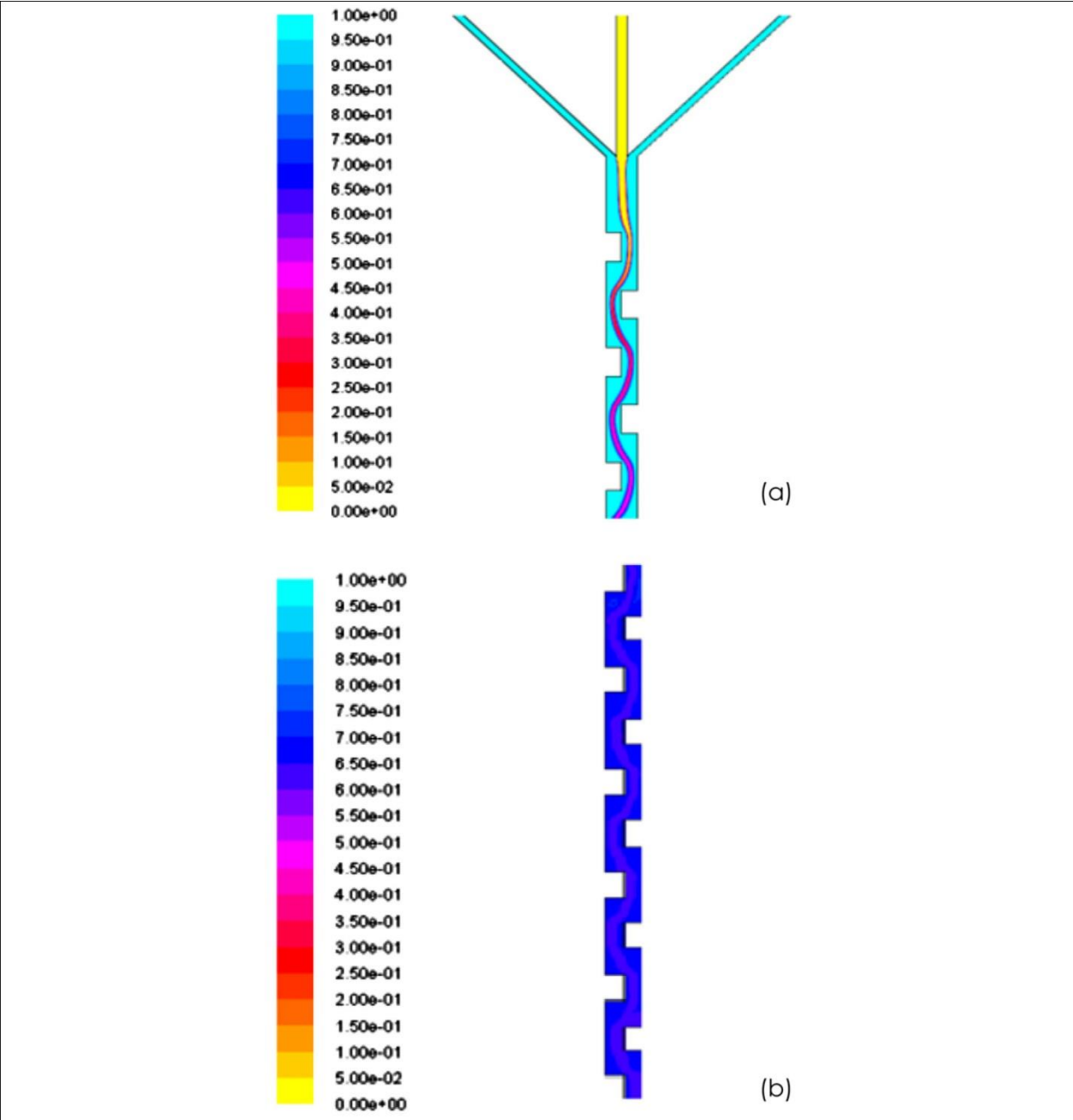


Fig. 3. Fluent results along the channel for Geometry 2, (a) in the entrance of the channel and (b) at the exit of the channel. Scale bar for mass fraction fluid 1 and fluid 2 are shown in the left.

Here swirling was not sufficient strong enough to help the mixing in early stage. Fig. 3b shows the mixing taking place along the central axis of the mixing channel at the outlet. Here noticeable mixing taking place in central line due to strong swirling effect. But near the channel wall, there is no significant mixing due to laminar flow [11]. Fig. 4a and b shows the mixing in the inlet and the outlet of the Geometry 3 which has a high mixing efficiency. The fluid starts to mix to a high degree early in this channel. Similar information can be observed in Figs. 5 and 6. Fig. 5 shows typical velocity vectors for three different geometries. In Geometry 1, there were no eddy currents created and all fluid travels straight down the channel length. The amount of diffusion taking place relies on the diffusion coefficients of the fluids being used.

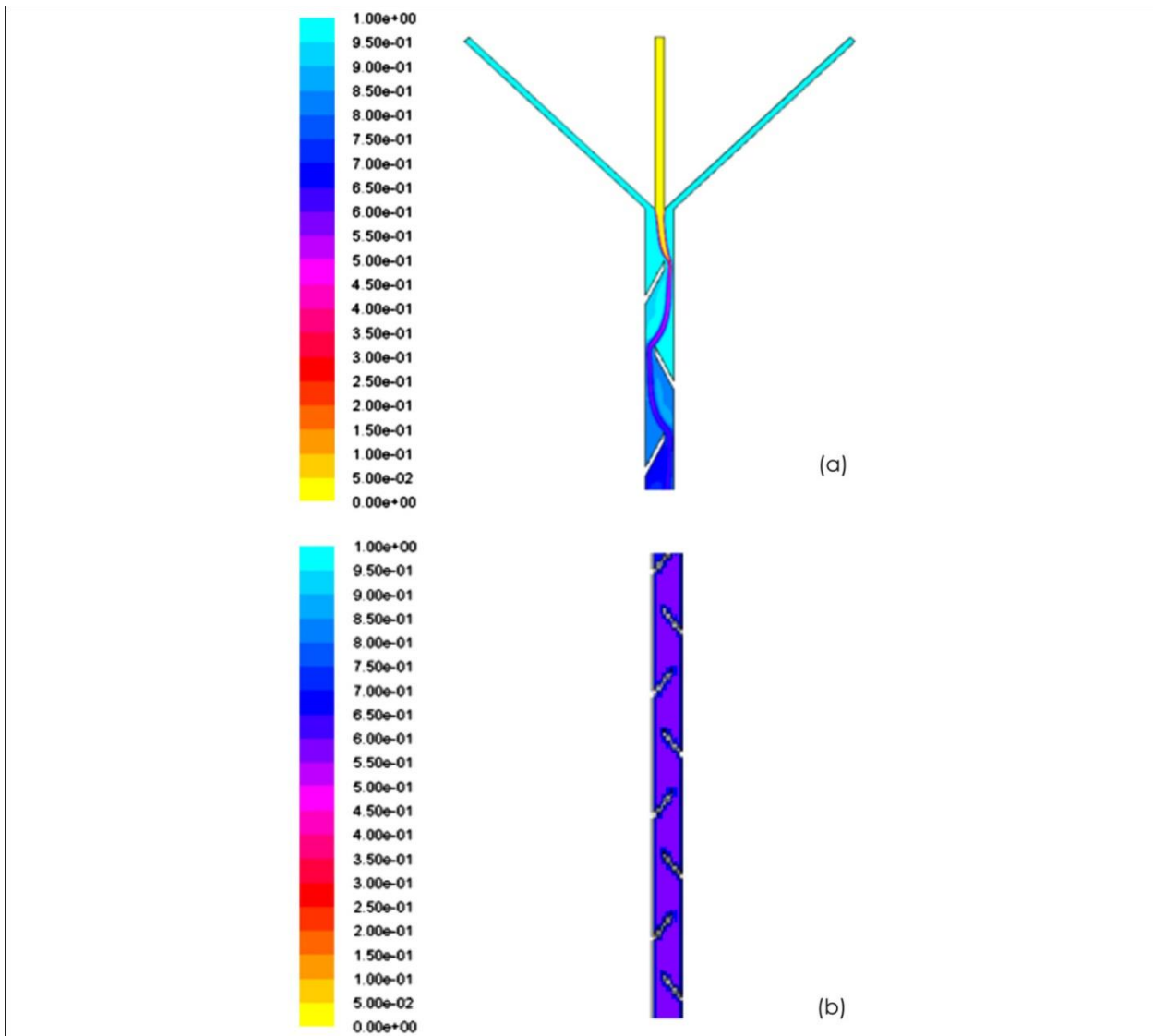


Fig. 4. Fluent results along the channel for Geometry 3, (a) in the entrance of the channel and (b) at the exit of the channel. Scale bar for mass fraction fluid 1 and fluid 2 are shown in the left.

Geometry 1 is poor for mixing and there was nothing to encourage mixing in the fluids that flow through it. In microchannel Reynolds number (Re) is calculated as $Re = (LV_{avg}\rho)/\mu$ ft, where L is the effective channel length, V , is the average velocity of fluid in the channel, ρ is the density and μ is the viscosity of the fluid. For this geometry the maximum Reynolds Number calculated was 110.

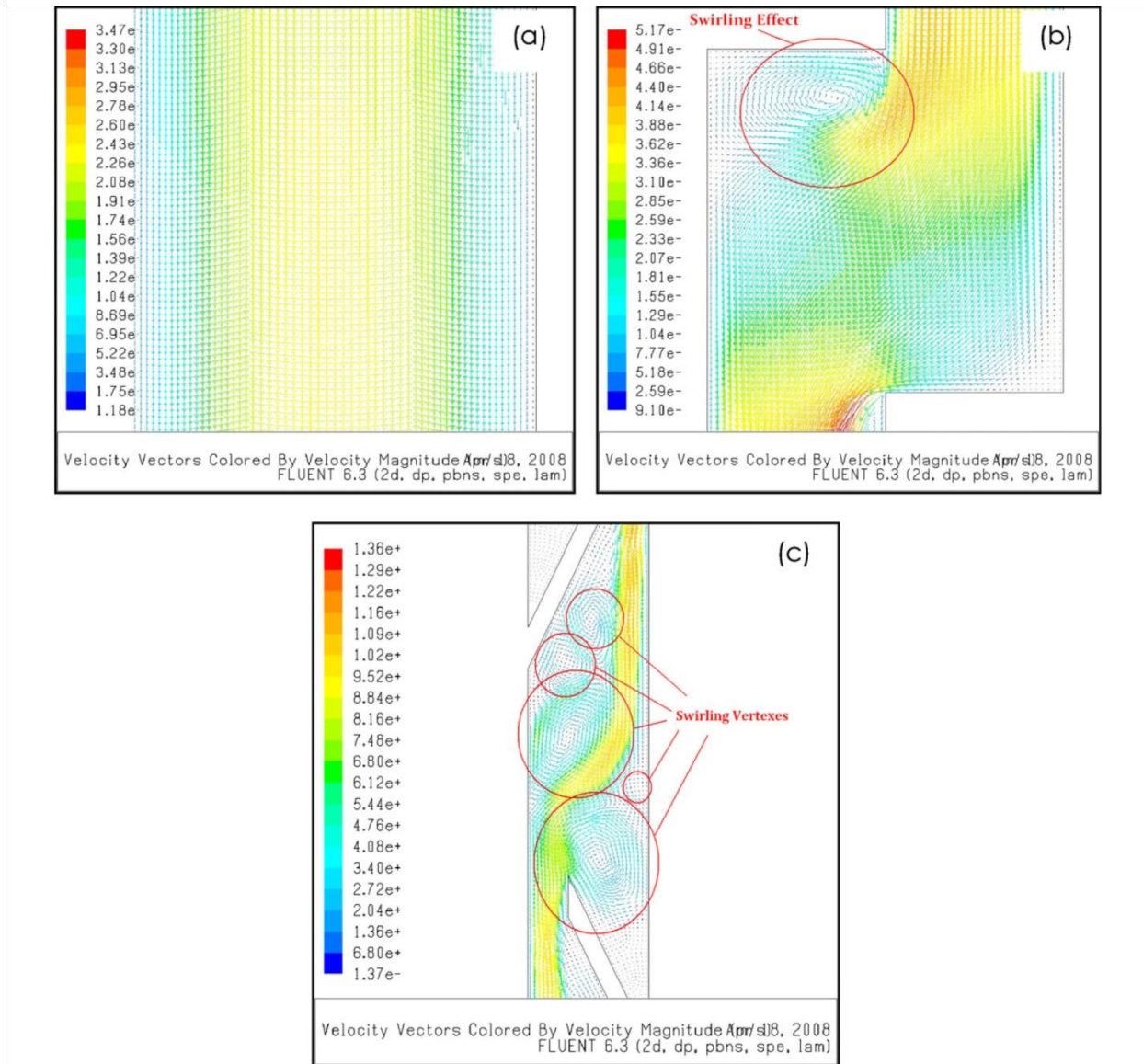


Fig. 5. Velocity vectors for (a) Geometry 1, (b) Geometry 2, and (c) Geometry 3. Scale of the velocity vectors are shown in the left hand side of each pictures.

Geometry 2 was chosen for this investigation as it contains a static mixing geometry contained in much published work [12]. The blocks are used to create swirling sections in the geometry. These swirling sections make the fluid travel back up the channel in a direction against the flow.

This opposing flow creates larger diffusion gradients resulting in more diffusion occurring. This idea of creating folding in the fluid to create better mixing has been reported in many papers [10,12]. It is described as the folding of the interface between the two unmixed streams [13]. The swirling vectors in this design have been responsible for an increase in its mixing performance seen in the simulation results (Fig. 2b).

Geometry 3 was designed with a view to creating as many swirling vortexes as possible. Fig. 5c shows, there are five separate swirling vortexes being created by the Geometry 3 which attributed to the superior mixing performance in the simulation results. This figure shown the fluid oscillates quite highly in the early channel sections due to the central stream coming from the central inlet being moved from side to side with the channel to navigate around the static mixers [14].

3.1. Mixing efficiency

Fig. 6 was generated using the mixing data obtained from the simulations. This figure agrees with the amount of mixing seen in Figs. 3 and 4 for Geometry 2 and 3. In Fig. 6a it is clearly shown that at the beginning in spite of having static barrier, efficiency of mixing was not improved much for Geometry 2. A small number of oscillations of mass fraction of two fluids were achieved around 33 mm and at the end of the channel a significant movement was observed. In that case, there would be a possibility to get a uniform mixing beyond the 50 mm length of the channel. In Geometry 3, the oscillations of mass fraction start in early stage and gradually increased their intensities. Higher oscillating intensity represents the swirling effect resulting the mixing efficiency which was achieved at around 45 mm channel length.

4. Conclusions

CFD models were successfully developed for three different microfluidic geometries. It was found that to achieve micro-fluidic mixing it is necessary to create swirling vortexes within the mixing geometry. Geometry 2 with blocks throughout the channels proved to be efficient in the modelling work. It is important that the vortex created will be within the fluid travelling through zone not in the dead zones seen in Geometry 3. Avoiding too much restriction in the microfluidic flow is important. Creating too much oppression to fluid flow leads to back pressures being created which may lead to lateral flow.

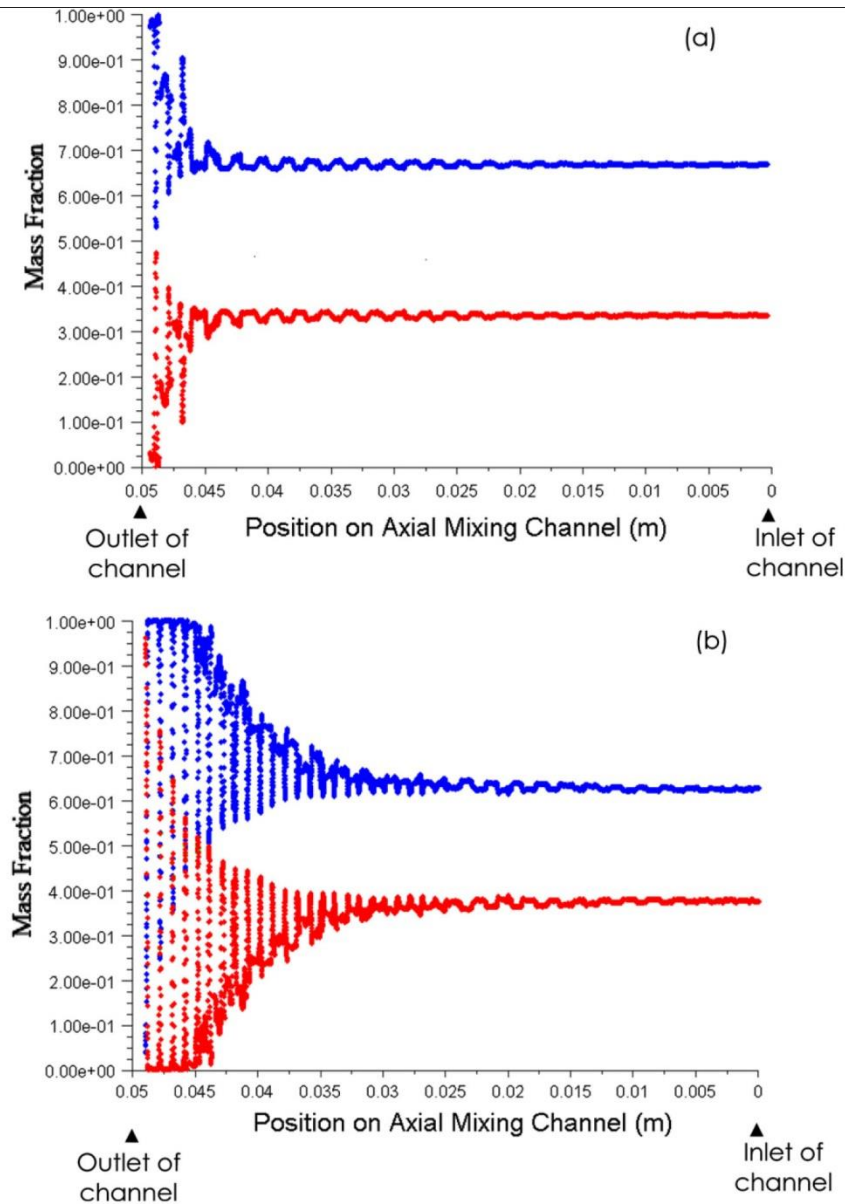


Fig. 6. Fluent results for (a) Geometry 2, (b) Geometry 3. Mass fraction of fluid 1 (♦) and fluid 2 (◆).

References

- [1] K. Samuel, M. George, Whiteside, microfluidic devices fabricated in poly(dimethylsiloxane) for biological studies, *Electrophoresis* 24 (2003) 3563-3576.
- [2] H.A. Stone, K. Kim, Microfluidics: basic issues, applications, and challenges, *AIChE Journal* 47 (6) (2001) 8.
- [3] Teruo Fujii, PDMS-based microfluidic devices for biomedical applications, *Microelectronic Engineering* 61-62 (2002) 907-914.

- [4] M.A. McClain, C.T. Culbertson, S.C. Jacobson, Nancy, L.C.E. Sims, J.M. Ramsey, Microfluidic devices for the high-throughput chemical analysis of cells, *Analytical Chemistry* 75 (21) (2003) 5646-5655.
- [5] M.Y. Ye et al, DNA separation with low-viscosity sieving matrix on microfabricated polycarbonate microfluidic chips, *Analytical and Bioanalytical Chemistry* 381 (2005) 820-827.
- [6] R. Kroger, CFD for Microfluidics, Fluent Deutschland GmbH, 2006. <<http://scai.fraunhofer.de/fileadmin/downloadifsi-biomedical/FSI-Bio-FluentKroeger.pdf>> (accessed 20.02.08).
- [7] D.M.L. Roberge, D.N. Bieler, Microreactor technology: a revolution for the chemical and pharmaceutical industries?, *Chemical Engineering & Technology* 28 (3) (2005) 318-323.
- [8] Fluent Inc, Introductory FLLUENT Notes, FLUENT v6.2, 2007.
- [9] Gambit 2.4.6, User Guide, Fluent Inc., Lebanon, New Hampshire, USA, 2007.
- [10] A. Dodge, M.C. Jullien, Y.K. Lee, X. Niu, F. Okkels, P. Tabeling, An example of a chaotic micromixer: the cross-channel micromixer, *CR Physique* 5 (2004) 557-563.
- [11] Robin H. Liu, Mark A. Stremler, Kendra V. Sharp, Michael G. Olsen, Juan G. Santiago, Ronald J. Adrian, Hassan Aref, David J. Beebe, Passive mixing in a three-dimensional serpentine microchannel, *Journal of Microelectromechanical Systems* 9 (2) (2000) 190-197.
- [12] S.H. Wong, P. Byrant, M. Ward, C. Wharton, Investigation of mixing in a cross-shaped micromixer with static mixing elements for reaction kinetics studies, *Sensors and Actuators* 95 (2003) 414-424.
- [13] P. Garstecki, M.A. Fischbach, G.M. Whitesides, Design for mixing using bubbles in branched microfluidic channels, *Applied Physics Letters* 86 (2005) 244108.
- [14] A.M. Elmabruk, Y.E. Mingxing, W. Yundong, D. Youyuan, A state-of-the-art review of mixing in microfluidic mixers, *Chinese Journal of Chemical Engineering* 16 (4) (2008) 503-516.